

## Spatial pattern of discrete and ultradiscrete Gray-Scott model

Matsuya, Keisuke

Department of Mathematical Engineering, Faculty of Engineering, Musashino University

<https://hdl.handle.net/2324/1566261>

---

出版情報 : MI lecture note series. 67, pp.48-53, 2016-02-05. 九州大学マス・フォア・インダストリ  
研究所  
バージョン :  
権利関係 :

# Spatial pattern of discrete and ultradiscrete Gray-Scott model

Keisuke Matsuya

Faculty of Engineering Department of Mathematical Engineering,  
Musashino University, Japan

(joint work with Mikio Murata)

## 1. INTRODUCTION

Discretization is a procedure to get difference equations with some parameters from given differential equations. The difference equations change to the differential equations with limits of the parameters. This procedure is often used when one computes differential equations numerically.

Ultradiscretization [1] is a limiting procedure transforming given difference equations into other difference equations which consist of addition, subtraction and maximum including cellular automata. In this procedure, a dependent variable  $u_n$  in a given equation is replaced by

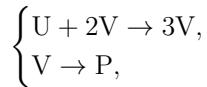
$$(1) \quad u_n = \exp\left(\frac{U_n}{\varepsilon}\right),$$

where  $\varepsilon$  is a positive parameter. Then, we apply  $\varepsilon \log$  to both sides of the equation and take the limit  $\varepsilon \rightarrow +0$ . Using identity

$$\lim_{\varepsilon \rightarrow +0} \varepsilon \log(e^{U/\varepsilon} + e^{V/\varepsilon}) = \max(U, V)$$

and exponential laws, we find that multiplication, division and addition for the original variables are replaced by addition, subtraction and maximum for the new ones, respectively. In this way, the original difference equation is approximated by a piecewise linear equation.

Gray-Scott model [2] is a variant of the auto catalytic model. Basically it considers the reactions



in an open flow reactor where U is continuously supplied, and the product P removed. A mathematical model of the reactions above is the following reaction-diffusion system:

$$(2) \quad \begin{cases} \frac{\partial u}{\partial t} = \Delta u - uv^2 + a(1 - u), \\ \frac{\partial v}{\partial t} = D_v \Delta v + uv^2 - bv, \end{cases}$$

where  $u := u(t, \vec{x})$ ,  $v := v(t, \vec{x})$ ,  $t \geq 0$ ,  $\vec{x} \in \mathbb{R}^d$  and  $D_v$ ,  $a$  and  $b$  are positive constants.  $\Delta$  is  $d$ -dimensional Laplacian. The solutions of this system represent spatial patterns. Changing not only an initial condition but also parameters, various patterns are observed [3, 4, 5].

In this talk, the speaker proposes a discretization and an ultradiscretization of the Gray-Scott model. The ultradiscrete system is directly related to the elementary cellular automata, especially Rule 90 which gives a Sierpinski gasket pattern [6].

## 2. DISCRETE GRAY-SCOTT MODEL

Since it is more convenient to consider the ultradiscretization, we take the scaling  $w := v + 1$  which changes (2) to

$$(3) \quad \begin{cases} \frac{\partial u}{\partial t} = \Delta u - u(w-1)^2 + a(1-u), \\ \frac{\partial w}{\partial t} = D_v \Delta w + u(w-1)^2 - b(w-1). \end{cases}$$

First we consider the discretization of following system of ordinary differential equations:

$$(4) \quad \begin{cases} \frac{du}{dt} = -u(w-1)^2 + a(1-u), \\ \frac{dw}{dt} = u(w-1)^2 - b(w-1), \end{cases}$$

where  $u := u(t)$ ,  $w := w(t)$ . We consider the following system of difference equations:

$$(5) \quad \begin{cases} u_{n+1} = \frac{u_n + \delta(2u_n w_{n+1} + a)}{1 + \delta\{(w_{n+1})^2 + a + 1\}}, \\ w_{n+1} = \frac{w_n + \delta[u_n\{(w_n)^2 + 1\} + b]}{1 + \delta(2u_n + b)}, \end{cases}$$

where  $n \in \mathbb{Z}_{\geq 0}$ ,  $\delta > 0$ . (5) is discretization of (4) and the method of discretization is same to that used in [6, 7]. Fixed points of (5) is same with (4) and stability of the fixed points of (5) is similar to those of (4) [6]. Using (5), we can construct a system of partial difference equations:

$$(6) \quad \begin{cases} \vec{w}_{n+1}^{\vec{j}} = \frac{m_p(\vec{u}_n^{\vec{j}}) + \delta(2m_p(\vec{u}_n^{\vec{j}})\vec{w}_{n+1}^{\vec{j}} + a)}{1 + \delta\{(\vec{w}_{n+1}^{\vec{j}})^2 + a + 1\}}, \\ \vec{w}_{n+1}^{\vec{j}} = \frac{m_q(\vec{w}_n^{\vec{j}}) + \delta\{m_p(\vec{u}_n^{\vec{j}})(m_q(\vec{w}_n^{\vec{j}})^2 + 1) + b\}}{1 + \delta(2m_p(\vec{u}_n^{\vec{j}}) + b)}, \end{cases}$$

where  $n \in \mathbb{Z}_{\geq 0}$ ,  $\vec{j} \in \mathbb{Z}^d$ ,  $p, q \in \mathbb{N}$ ,

$$m_p(\vec{u}_n^{\vec{j}}) := \sum_{k=1}^d \frac{u_n^{\vec{j}+p\vec{e}_k} + u_n^{\vec{j}-p\vec{e}_k}}{2d}, \quad m_q(\vec{w}_n^{\vec{j}}) := \sum_{k=1}^d \frac{w_n^{\vec{j}+q\vec{e}_k} + w_n^{\vec{j}-q\vec{e}_k}}{2d}$$

and  $\vec{e}_k \in \mathbb{Z}^d$  is a unit vector whose  $k$ th component is 1. Since (6) is equivalent to

$$\begin{cases} \frac{\vec{w}_{n+1}^{\vec{j}} - \vec{w}_n^{\vec{j}}}{\delta} = \sum_{k=1}^d \frac{u_n^{\vec{j}+p\vec{e}_k} - 2u_n^{\vec{j}} + u_n^{\vec{j}-p\vec{e}_k}}{(p\xi)^2} - m_p(\vec{u}_n^{\vec{j}})(\vec{w}_{n+1}^{\vec{j}} - 1)^2 \\ \quad + a(1 - m_p(\vec{u}_n^{\vec{j}})) + o(\delta), \\ \frac{\vec{w}_{n+1}^{\vec{j}} - \vec{w}_n^{\vec{j}}}{\delta} = \frac{q^2}{p^2} \sum_{k=1}^d \frac{w_n^{\vec{j}+q\vec{e}_k} - 2w_n^{\vec{j}} + w_n^{\vec{j}-q\vec{e}_k}}{(q\xi)^2} + m_p(\vec{u}_n^{\vec{j}})(m_q(\vec{w}_n^{\vec{j}}) - 1)^2 \\ \quad - b(m_q(\vec{w}_n^{\vec{j}}) - 1) + o(\delta), \end{cases}$$

where  $\xi := \sqrt{2d\delta}/p$ , if there exists smooth functions  $u(t, \vec{x})$ ,  $w(t, \vec{x})$  ( $t \geq 0$ ,  $\vec{x} \in \mathbb{R}^d$ ) that satisfy  $u(\delta n, \xi \vec{j}) = u_n^{\vec{j}}$  and  $w(\delta n, \xi \vec{j}) = w_n^{\vec{j}}$ , we obtain (3) where  $D_v = (q/p)^2$  with the limit  $\delta \rightarrow 0$ .

Now, let spatial dimension  $d = 1$  and  $p = 3$ ,  $q = 1$ ,  $\delta = 0.1$  and

$$u_0^j = \begin{cases} 1 - 0.3 \cos\left(\frac{\pi j}{50}\right) & |j| \leq 25 \\ 1 & |j| > 25 \end{cases}, \quad w_0^j = \begin{cases} 1 + 0.5 \cos\left(\frac{\pi j}{50}\right) & |j| \leq 25 \\ 1 & |j| > 25 \end{cases}.$$

If one plots the solutions of (6) with a periodic boundary condition, the following patterns are observed. The horizontal axis is for space variable  $j$ . The vertical axis is for time variable  $n$ . We get contour plots of the values for  $w_n^j$ .

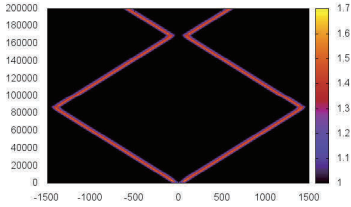


FIGURE 1.  $a = 0.03$ ,  $b = 0.10$

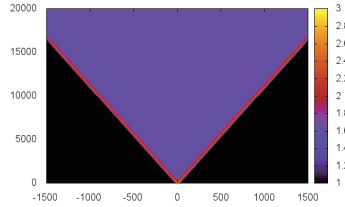


FIGURE 2.  $a = 0.04$ ,  $b = 0.06$

In Figure 1, a peak split into two peaks and two peaks move opposite side. We took a periodic boundary condition so that it is observed that two peaks pass each other. In Figure 2, a similar situation of Figure 1 is observed. Between two peaks, values of  $(u, w)$  converge to the stable equilibrium point  $P_{d,+}$ . Since we take periodic boundary conditions, two peaks collide at the boundary and vanish.

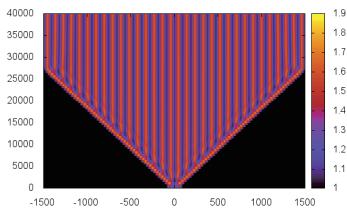


FIGURE 3.  $a = 0.04$ ,  $b = 0.09$

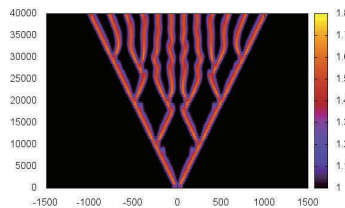


FIGURE 4.  $a = 0.04$ ,  $b = 0.11$

In Figure 3 and 4, a peak split into two peaks several times and a self-replicating pattern is observed.

### 3. ULTRADISCRETE GRAY-SCOTT MODEL

Let

$$u_n^{\vec{j}} = \exp\left(\frac{U_n^{\vec{j}}}{\varepsilon}\right), \quad w_n^{\vec{j}} = \exp\left(\frac{W_n^{\vec{j}}}{\varepsilon}\right),$$

$$\delta = \exp\left(\frac{D}{\varepsilon}\right), \quad a = \exp\left(\frac{A}{\varepsilon}\right), \quad b = \exp\left(\frac{B}{\varepsilon}\right)$$

and take the limit  $\varepsilon \rightarrow +0$ , then we have

$$(7) \quad \begin{cases} U_{n+1}^{\vec{j}} = \max[M_p(U_n^{\vec{j}}), D + \max[M_p(U_n^{\vec{j}}) + W_{n+1}^{\vec{j}}, A]] \\ \quad - \max[0, D + \max[2W_{n+1}^{\vec{j}}, A, 0]], \\ W_{n+1}^{\vec{j}} = \max[M_q(W_n^{\vec{j}}), D + \max[M_p(U_n^{\vec{j}}) + \max[2M_q(W_n^{\vec{j}}), 0], B]] \\ \quad - \max[0, D + \max[M_p(U_n^{\vec{j}}), B]], \end{cases}$$

where

$$M_p(U_n^{\vec{j}}) := \max_{k=1, \dots, d} [U_n^{\vec{j}+p\vec{e}_k}, U_n^{\vec{j}-p\vec{e}_k}],$$

$$M_q(W_n^{\vec{j}}) := \max_{k=1, \dots, d} [W_n^{\vec{j}+q\vec{e}_k}, W_n^{\vec{j}-q\vec{e}_k}].$$

Taking a limit  $D \rightarrow \infty$  and assuming  $W_n^{\vec{j}} \geq 0$ , then (7) changes to

$$(8) \quad \begin{cases} U_{n+1}^{\vec{j}} = \max[M_p(U_n^{\vec{j}}) + W_{n+1}^{\vec{j}}, A] - \max[2W_{n+1}^{\vec{j}}, A], \\ W_{n+1}^{\vec{j}} = \max[M_p(U_n^{\vec{j}}) + 2M_q(W_n^{\vec{j}}), B] - \max[M_p(U_n^{\vec{j}}), B]. \end{cases}$$

Let spatial dimension  $d = 1$  and initial data of (8)  $-U_0^j \in \{0, 1\}$ ,  $W_0^j \in \{0, 1\}$ . Taking some conditions to parameters  $A$  and  $B$ , the solution of (8) becomes to a cellular automaton. There are five types of the conditions for  $A$  and  $B$  as follow:

Type I	Type II	Type III	Type IV	Type V
$A \leq -1$	$0 \leq A \leq 1$	$A \geq 2$	$A \leq -1$	$A \geq 0$
$B = 1$	$B = 1$	$B = 1$	$B \geq 2$	$B \geq 2$

Type I: The rule for  $A \leq -1$ ,  $B = 1$ :

$$\begin{array}{c|c|c|c|c} -M_p(U_n^j), M_q(W_n^j) & 1, 1 & 1, 0 & 0, 1 & 0, 0 \\ \hline -U_{n+1}^j, W_{n+1}^j & 1, 0 & 1, 0 & 1, 1 & 0, 0 \end{array}$$

In this case, we can observe the patterns in Figure 5. Values of  $W_n^j$  is represent as

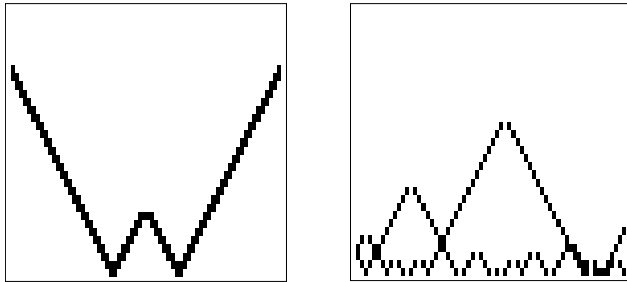


FIGURE 5.  $W_n^j$  with  $A = -1$ ,  $B = 1$  and  $p = q = 1$ .

follow: 0 (white) and 1 (black). The horizontal axis is for space variable  $j$ . The vertical axis is for time variable  $n$ . Time evolution started from two peaks in the left side and from several peaks in the right side. In Figure 5, every peaks split into two peaks and move opposite side. Two peaks vanish, when they collide.

Type II: The rule for  $0 \leq A \leq 1, B = 1$ :

$$\frac{-M_p(U_n^j), M_q(W_n^j)}{-U_{n+1}^j, W_{n+1}^j} \left| \begin{array}{c|c|c|c} 1, 1 & 1, 0 & 0, 1 & 0, 0 \\ \hline 0, 0 & 0, 0 & 1, 1 & 0, 0 \end{array} \right.$$

In this case,  $U_{n+1}^j = -W_{n+1}^j$  and we can observe the patterns in Figure 6 and 7. Since this relation is held,  $W_n^j$  satisfies a single equation. Moreover, taking  $p = q = 1$ , the equation is same as ECA rule 90, which is well known for fractal design:

$$\frac{W_n^{j-1} W_n^j W_n^{j+1}}{W_{n+1}^j} \left| \begin{array}{c|c|c|c|c|c|c|c} 111 & 110 & 101 & 100 & 011 & 010 & 001 & 000 \\ \hline 0 & 1 & 0 & 1 & 1 & 0 & 1 & 0 \end{array} \right.$$

In Figure 6 and 7, time evolution started from two peaks in the left sides and from

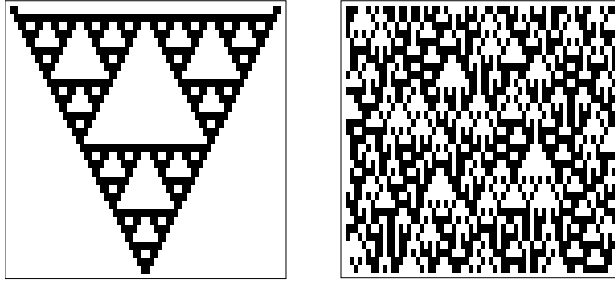


FIGURE 6.  $W_n^j$  with  $A = 0, B = 1$  and  $p = q = 1$ .

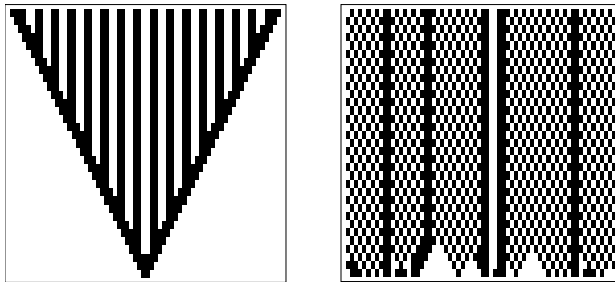


FIGURE 7.  $W_n^j$  with  $A = 0, B = 1, p = 2$  and  $q = 1$

several peaks in the right sides. In the left side of Figure 6, Sierpinski gasket pattern is observed.

Type III: The rule for  $A \geq 2, B = 1$ :

$$\frac{-M_p(U_n^j), M_q(W_n^j)}{-U_{n+1}^j, W_{n+1}^j} \left| \begin{array}{c|c|c|c} 1, 1 & 1, 0 & 0, 1 & 0, 0 \\ \hline 0, 0 & 0, 0 & 0, 1 & 0, 0 \end{array} \right.$$

In this case,  $U_{n+1}^j = 0$  so that  $W_n^j$  satisfies  $W_{n+1}^j = M_q(W_n^j)$ .

Type IV: The rule of  $A \leq -1, B \geq 2$ :

$$\frac{-M_p(U_n^j), M_q(W_n^j)}{-U_{n+1}^j, W_{n+1}^j} \left| \begin{array}{c|c|c|c} 1, 1 & 1, 0 & 0, 1 & 0, 0 \\ \hline 1, 0 & 1, 0 & 0, 0 & 0, 0 \end{array} \right.$$

In this case,  $W_{n+1}^j = 0$  so that  $U_n^j$  satisfies  $U_{n+1}^j = M_p(U_n^j)$ .

Type V: The rule of  $A \geq 0, B \geq 2$ :

$$\frac{-M_p(U_n^j), M_q(W_n^j)}{-U_{n+1}^j, W_{n+1}^j} \left| \begin{array}{c|c|c|c} 1, 1 & 1, 0 & 0, 1 & 0, 0 \\ \hline 0, 0 & 0, 0 & 0, 0 & 0, 0 \end{array} \right.$$

In this case,  $U_{n+1}^j = W_{n+1}^j = 0$  so that  $U$  and  $W$  vanish immediately.

#### 4. CONCLUDING REMARKS

In this abstract, we proposed and investigated discrete and ultradiscrete Gray-Scott model, which is a two component reaction diffusion system. We found that solutions of each equation reveal various spatial patterns. Moreover, there are solutions of the discrete equation and the ultradiscrete equation whose solutions give similar spatial patterns. The ultradiscrete Gray-Scott model has a solution which is an elementary cellular automaton and which reveals Sierpinski gasket. The method of discretization and ultradiscretization of Gray-Scott in this paper is one method to relate reaction diffusion systems to cellular automata. Clarifying the relation between solutions of discrete Gray-Scott model and those of ultradiscrete Gray-Scott model is a future work for the authors.

#### ACKNOWLEDGMENTS

The authors are deeply grateful to Prof. Tetsuji Tokihiro who provided helpful comments and suggestions. This work was supported by JSPS KAKENHI Grant Number 23740125.

#### REFERENCES

- [1] T. Tokihiro, D. Takahashi, J. Matsukidaira and J. Satsuma, From soliton equations to integrable cellular automata through a limiting procedure, *Phys. Rev. Lett.* 29 (1996), 3247–3250
- [2] P. Gray and S. K. Scott, Sustained oscillations and other exotic patterns of behaviour in isothermal reactions, *J. Phys. Chem.* 89 (1985), 22–32
- [3] W. Mazin, K. E. Rasmussen, E. Mosekilde, P. Borckmans and G. Dewel, Pattern formation in the bistable Gray-Scott model, *Math. Comput. Simul.* 40 (1996), 371–396
- [4] Y. Nishiura and D. Ueyama, A skeleton structure of self-replicating dynamics, *Physica D* 130 (1999), 73–104
- [5] Y. Nishiura and D. Ueyama, Spatio-temporal chaos for the Gray-Scott model, *Physica D* 150 (2001), 137–162
- [6] K. Matsuya and M. Murata, Spatial pattern of discrete and ultradiscrete Gray-Scott model, *Discrete Contin. Dyn. Syst. Ser. B* 20 (2015), 173–187
- [7] M. Murata, Tropical discretization: ultradiscrete Fisher-KPP equation and ultradiscrete Allen-Cahn equation, *J. Difference Equ. Appl.* 19 (2013), 1008–1021